Dynamic plant height QTL revealed in maize through remote sensing phenotyping using a high-throughput unmanned aerial vehicle (UAV)

Xiaqing Wang[1,5], Ruyang Zhang[1,5], Liang Han[2,3,5], Hao Yang[2], Wei Song[1], Xiaolei Liu[4], Xuan Sun[1], Meijie Luo[1], Kuan Chen[1], Yunxia Zhang[1], Guijun Yang[2,*], Yanxin Zhao[1,*], Jiuran Zhao[1,*]

[1] Beijing Key Laboratory of Maize DNA Fingerprinting and Molecular Breeding, Maize Research Center, Beijing Academy of Agriculture & Forestry Sciences, Beijing 100097, China

[2] Key Laboratory of Quantitative Remote Sensing in Agriculture of Ministry of Agriculture, Beijing Research Center for Information Technology in Agriculture, Beijing 100097, China.

[3] College of Architecture and Geomatics Engineering, Shanxi Datong University Datong, Datong 037009, China.

[4] Key Laboratory of Agricultural Animal Genetics, Breeding and Reproduction, Ministry of Education, College of Animal Science and Technology, Huazhong Agricultural University, Wuhan 430070, Hubei, China .

[5] These authors contributed equally to this work.

[*] To whom correspondence should be addressed. Tel: 0086-010-51502407; guijun.yang@163.com or rentlang2003@163.com or maizezhao@126.com.

Running title: Dynamic plant height revealed by unmanned aerial vehicle

Highlight

We used UAV-based sensing platform to investigate plant height over 4 growth stages for different maize populations, and detected numbers of reliable QTLs using GWAS.

Abstract

Plant height is the key factor for plant architecture, biomass and yield in maize (*Zea mays*). In this study, plant height was investigated using unmanned aerial vehicle high-throughput phenotypic platforms (UAV-HTPPs) for maize diversity inbred lines at four important growth stages. Using an automated pipeline, we extracted accurate plant heights. We found that in temperate regions, from sowing to the jointing period, the growth rate for temperate maize was faster than tropical maize. However, from jointing to flowering stage, tropical maize maintained a vigorous growth state, and finally resulted in a taller plant than temperate lines. Genome-wide association study for temperate, tropical and both groups identified a total of 238 quantitative trait locus (QTLs) for the 16 plant height related traits over four growth periods. And, we found that plant height at different stages were controlled by different genes, for example, *PIN1* controlled plant height at the early stage and *PIN11* at the flowering stages. In this study, the plant height data collected by the UAV-HTTPs were credible and the genetic mapping power is high, indicating that the application of this UAV-HTTPs into the study of plant height will have great prospects.

Key words: Dynamic plant height, GWAS, High-throughput phenotype, QTL, Temperate maize, Tropical maize, Unmanned aerial vehicle.

Abbreviations

BOTH, Both of temperate and tropical maize; CSMs, Crop surface models; CV, Coefficient of variation; DEM, Digital elevation model; DGRPH, Daily growth rate of plant height; DIPH, Daily incremental plant height; DSMs, Digital surface models; EGI, Excess Green Index; GCPs, Ground control points; GPS, Global positioning system; GRPH, Growth rate of plant height; IPH, Incremental plant height; MAF, Minor allele frequency; PH, Plant height; QTL, Quantitative trait locus; SNP, Single nucleotide polymorphism; TEM, Temperate maize; TST, Tropical maize; UVA, Unmanned aerial vehicle; UAV-HTPPs, Unmanned aerial vehicle high-throughput phenotypic platforms

Introduction

Maize (*Zea mays*) was domesticated from Balsas teosinte (*Zea mays* subspecies *parviglumis*) in southwestern Mexico around 9,000 y BP (van Heerwaarden et al., 2011). Subsequently, maize has been continuously improved by humans, and the most important improvements were spread from the tropical region to the temperate region, which can be called adaptation (Liu et al., 2015). The adaptation process allowed maize to be widely cultivated worldwide and become the largest production food crop in the world (http://faostat3.fao.org/compare/E). However, the world population is soaring and the demand for food is also increasing. It has been reported that the world's grain demand must meet a target of 70% increase by 2050 (Tester and Langridge, 2010). Therefore, corn, the largest grain, has become particularly important in safeguarding world food security.

Maize yield is highly complex and is affected by many factors, among which plant height is a particularly important factor because it not only affects the lodging resistance, but also biomass and yield (Salas Fernandez 2009). In the first Green Revolution, with the successful application of the semi-dwarf genes (*rht1*; *sd1*) in wheat and rice, the crop yields increased dramatically (Peng et al., 1999; Khush et al., 2001; Sasaki et al., 2002). Plant height was so important that people have made unremitting efforts to exploring its genetic mechanism. So far, there were plenty of quantitative trait loci (QTLs) identified for maize plant height using a diversity of genetic populations (Peiffer et al., 2014; Yang et al., 2014; Dell'Acqua et al., 2015; Zhou et al., 2016; Pan et al., 2017). Some of these genes were cloned, such as *an1*, *dwarf3*, *dwarf8*, *dwarf9* and *br2*, which were mainly involved in the synthesis and transportation of gibberellin and auxin (Winkler and Freeling, 1994; Bensen et al., 1995; Winkler et al., 1995; Fujioka et al., 1988; Xing et al., 2012).

Maize plant height showed different characteristics during the whole growth period, especially in the important growth stages, such as the seeding, jointing, flowering and mature stages (Abendroth et al., 2011). Usually, maize grows slowly in the seedling stage, fast in the jointing stage, then gradually slower in the grouting stage, and stops in the milky stage (Zhang et al., 2012). However, for a long time, researchers have often investigated the plant height at the mature stage to obtain the final height, leading to a lack of systemic understanding of the entire plant height development process and the genetic factors of its genetic development mechanism. Furthermore, the workload of manual measurement also contributed to plant height

typically only being investigated at one growth stage.

Manually investigating plant height is a laborious and time-consuming task. Since plants are tall at maturity, errors are unavoidable in the measurement process and the accuracy of the data will be affected. In recent years, with the development of artificial intelligence, a series of high-throughput automated phenotypic systems have been developed. At present, indoor platform systems are widely used for dissecting phenotypic traits in which environmental effects are minimized (Yang et al., 2014; Zhang et al., 2016; Al-Tamimi et al., 2017); however, field high-throughput platforms have much fewer applications within the complex environment that farmers routinely experience (Crain et al., 2016; Liang et al., 2018). Compared with indoor platforms, the development of field high-throughput platforms requires high flexibility and a large payload (Araus and Cairns, 2014). Thanks to the advance in remote sensing, aeronautics and high-performance computing development, some field-based high-throughput phenotypic platforms (HTPPs) have been developed (Araus and Cairns, 2014). For example, the Australian Plant Phenomics Facility (http://www.plantphenomics.org/hrppc/capabilities/technology), and ground-based HTPPs used for wheat, cotton, sorghum and maize, which can determine the canopy height, reflectance, temperature, plant height, biomass and so on (Andrade-Sanchez et al., 2013; Holman 2016; Duan et al., 2017; Liang et al., 2018). However, these field-based HTPPs have very few applications in genetic improvement, especially for genetic mapping.

To better understand the dynamic plant height mechanism, we investigated the plant height through four growth periods with an unmanned aerial vehicle (UAV) system for maize diversity inbred lines, which covers wide genetic diversity and is widely used in maize genetic research (Yang et al., 2011; Yang et al., 2014; Liu et al., 2017). Through this design, we hope to explore more plant height characteristics with the aid of the high-throughput UAV and data processing procedures, and then dissect the genetic basis for plant height for different maize groups at different stages.

Materials and methods

Plant materials and experiment design

The maize natural population used in this study was a subset of Yang (Yang et al., 2010), consisting of 117 temperate lines and 135 tropical lines, which had a high-density genotype of 1.25 million single nucleotide polymorphism (SNPs) with

minor allele frequency (MAF) more than 0.05 (Liu et al., 2017). The population was sown on 15 May 2017 at Xiao Tang Shan, Changping, Beijing National Precision Agriculture Research Center of China (115°E, 40°N). The land plots were flat, with uniform soil fertility. There was a row length of 2 m, including eight plants, and each line included three rows. Row-to-row distance was set as 65 cm. Phenotypic data collection with UAV was carried out on 8 June, 29 June, 11 July and 3 August 2017, days with clear sky and no wind (Table 1; Fig. 1A). On the same days, the height of 44 randomly selected plants was manually measured with a ruler.

Platform and image acquisition

An Octocopter UAV (DJI Spreading Wings S1000) platform was used to collect a set of aerial images across four flights (Fig. 1B). A 20.2-megapixel digital camera (Cyber-shot DSC-QX100) was mounted on the UAV to acquire the images by means of a global positioning system (GPS) and inertial navigation unit system. In each flight, the same flight plan was followed with 80% forward overlap and 75% side overlap at an altitude of approximately 40–60 m, depending on the sun situation. The flight routes were programmed into the UAV software to automatically generate efficient flight paths for UAV. Each flight speed was set to 6 m/s. International Standards Organization sensitivity and shutter speed were set to automatic, and the focal length was fixed at 10.4 mm. The flight time was within 15 min. Sixteen ground control points (GCPs), measured using millimeter-accuracy differential GPS (South Surveying & Mapping Instrument Co., Ltd., China), were evenly distributed in the field to obtain an accurate geographical reference from multiple dates.

Plant height image data extraction and verification

Digital surface models (DSMs) and orthomosaics were produced from images shot by UAV with GCPs using the structure-from-motion software Agisoft PhotoScan 1.3 (Agisoft LLC, St. Petersburg, Russia) (Fig. 1B). This process included feature point matching, dense point cloud generation, product output, etc. A digital elevation model (DEM) (i.e., a non-vegetation ground model) was constructed from the first set of aerial images collected 24 days after sowing by the local polynomial interpolation method. Crop surface models (CSMs) were calculated by subtracting the DSM at different plant growth stages from the DEM (Fig. 1B, Hoffmeister et al., 2010; Bendig et al., 2013; Hoffmeister et al., 2013). The CSM includes a raster dataset that mixes

the soil and plant pixels. Many studies have shown that extracting plant height directly from CSM results in underestimation (Bendig et al., 2015; Holman et al., 2016; Watanabe et al., 2017). Segmenting plants from soils using the excess green index proposed by Woebbecke et al. (1995) was a necessary measure for the above extraction. Kriging spatial interpolation and maximum adjacent pixel methods were performed on CSMs to remove the soil background, and the maximum of interpolation was taken as the representative value of plant height at the plot scale. To assess the accuracy of plant height extraction from UAV, 44 maize plants were randomly selected to manually measure plant height at the second, third and fourth timepoints of plant growth. A linear regression model was applied with multiple dates using R v. 3.2.4 statistical software.

Plant height variation between temperate and tropical maize

A total of 252 maize inbred lines, consisting of 117 temperate lines and 135 tropical lines, were used in this study. Plant heights were evaluated at four different growth stages, and a total of 16 plant height related traits were calculated, including 4 absolute plant height traits (PH), 3 incremental plant height difference (IPH), 3 growth rates of plant height (GRPH), 3 daily incremental plant height difference (DIPH) and 3 daily growth rates of plant height (DGRPH). The PH represents the absolute plant height at each timepoint. The IPH represents the difference between the adjacent timepoints, e.g. IPH_1t2 equals PH_2 minus PH_1. The GRPH was calculated as the ratio of IPH divided by the former plant height, e.g. GRPH_1t2 equals IPH_1t2 divided by PH_1. The DIPH was the IPH divided by the total days between the adjacent timepoints. Finally, the DGRPH was calculated as the GRPH divided by the total days between the adjacent timepoints. The phenotypic distribution and graphs were implemented in the R v. 3.2.4 statistical software.

Association analysis for plant height

Genome-wide association study (GWAS) was carried out in temperate (TEM), tropical (TST) maize and both of the two e population (BOTH). Genotype data quality control was performed separately, with 1,141,328, 1,110,483 and 1,227,441 SNPs remaining for TEM, TST and BOTH groups, respectively. We used 16 plant-height-related traits in the GWAS program, including PH, IPH, GRPH, DIPH and DGRPH traits for the three groups. Combined with phenotypes and genotypes,

the FarmCPU model in the MVP software package, which iteratively uses fixed and random effect model, was used for association tests in TEM and TST groups with only kinship considered (Al-Tamimi et al., 2016; Liu et al., 2016). For the BOTH population, the top five principal components were added in FarmCPU model to control false positives, which may be caused by population stratification and the non-genetic effect (Al-Tamimi et al., 2016; Liu et al., 2016). The adjusted Bonferroni method (i.e., $P \leq 1/N$, where N is the total number of genome-wide SNPs) was used as the global P value cutoff to declare significance of SNPs associated with a given trait. The P values were 8.76e−7, 9.0e−7 and 8.14e−7 for the TEM, TST and BOTH populations, respectively. QTL intervals were calculated as the upstream and downstream 100kb for each significant SNP (Deng et al., 2017). Any SNP in the QTL interval with the lowest *P* value was considered as the peak SNP.

We searched the genes in each QTL according to the physical position of each gene in maizeGDB (https://www.maizegdb.org/). Gene annotations were based on both maizeGDB and InterProScan database (http: //www. ebi.ac.uk/interpro/scan.html). The gene expression profiles were also from maizeGDB.

Results

High-throughput digital plant height extraction and validation

To investigate the plant height of 117 temperate and 135 tropical maize inbred lines for the four stages, we used the unmanned aerial vehicle high-throughput phenotypic platform (UAV-HTTP) system to collect the image data. We carried out four flights during the whole development stage of maize during the seedling, jointing, trumpet and flowering periods (the V5, V10, V12 and R stages at 24, 45, 57 and 80 days after seeding, respectively). On each flight, the average flight altitude was 52.5 m. A total of 559 original images were taken on four flights (Table 2). Using the self-developed automated data extraction process, we first filtered the original images, and retained 460 high-quality images, with an average of 115 images per flight. After the reconstruction of the orthomosaic model, the obtained image ground resolution was 1.15 cm/pixel. The DSM was constructed using the orthomosaic model output point cloud data. The average image accuracy of the DSM was 2.31 cm/pixel. The DEM was generated by interpolation of the DSM points located on the surface of the

bare land. Finally, we obtained the CSM containing bare soil (DSM − DEM, Fig. 1B). Here, the tiny terrain at the bottom of the crop can be ignored because whole plant area was flatted by a farmland leveling machine. Therefore, CSM is equivalent to crop height. The average coefficient of variation (CV) of plant height gradually decreased from 53% to 11.6% among first three growth stages caused by the increasing heterogeneity of plant height. The mean crop height ranged from 9.6 to 253.4 cm among the four periods with an average growth rate of 4.06 cm/d (Table 2).

To verify the accuracy of the plant height data extracted using UAV-HTTP, 44 lines were randomly selected for plant height measurement by ruler at the same time as the 2nd, 3rd and 4th flight. A linear regression model was established for the UAV-HTTP data and ruler measurement data and the model correlation coefficient was very high (r^2= 0.91), indicating that the data obtained by the UAV platform had high accuracy (Fig. 2).

Plant height varies greatly at different stages of development

Based on the accurate plant height data obtained by UAV-HTTP, we performed further analysis of the variation for maize plant height across the four growth stages among the three different groups (Table 3). For the BOTH group, the average PH were between 13.66 and 218.26 cm, from the first to the fourth flight (Fig. 1C). The DIPH values for the three adjacent periods were from 3.68 to 4.74 cm, with the maximum for 2t3 stages, and minimum for 3t4 stages. However, the DGRPH values varied from 0.02 to 0.31, with the maximum for 1t2 stages, and minimum for 3t4 stages. The inconsistence for DIPH and DGRPH indicate that growth rate was not positively correlate to incremental growth.

We conducted a correlation analysis for the BOTH group to reveal the relationship between the 16 traits at different plant stages (Fig. 3). A strong positive correlation was found between IPH and DIPH, GRPH and DGRPH. Second, correlations for PHs at different stages were also positively related, from 0.14 to 0.73. Third, the correlation between IPHs was weak ranging from −0.25 to 0.05. PHRs were also weakly related to each other, from −0.09 to 0.1. However, there was a positive correlation between IPH and PH, ranging from −0.28 to 0.94. The correlation between GRPH and PH was mainly negative, ranging from −0.73 to 0.62. In addition, the correlation between IPH and GR was relatively variable, ranging from −0.57 to 0.95.

As the wide diversity of the BOTH group, we divided the group into TEM and TST groups, and found the plant height between TEM and TST maize exhibited a significant difference at each growth stage (Fig. 4). From the first to the third flight (namely 1t2 and 2t3 stages) the DIPH values for TEM and TST were 3.87 vs. 3.52 cm and 4.97 vs. 4.53 cm, respectively, showing that TEM maize consistently grew faster than the TST maize. However, from the third to the fourth period, the TST grew faster than the TEM maize, and the DIPH for TEM and TST were 2.32 vs. 3.79 cm. More importantly, the most significant difference for the two groups were at 3t4 stage when most TEM lines were flowering, while most TST lines were still in vegetative growth.

Genetic basis affecting the dynamic development of plant height

In view of the above-mentioned differences in plant height and related traits in different groups and at different stages of growth, we conducted GWAS for the 16 plant heigt related traits in the TEM, TST, and BOTH groups. A total of 238 QTLs were detected, covering 10 chromosomes of the maize genome (Data S1-S5; Fig. S1-S4). There were 38, 49, 50, 50 and 51 QTLs detected for PH, IPH, GRPH, DIPH and DGRPH traits, respectively.

To verify the accuracy of the QTL, we compared the previously reported QTLs and genes related to plant height and found that 45% of the QTLs overlapped with previous research (Peiffer et al., 2014; Yang et al., 2014; Dell'Acqua et al., 2015; Zhou et al., 2016; Pan et al., 2017). In addition, genes involving the GA and auxin pathway were also detected to be associated with plant height, such as *ARFTF4*, *D3*, *GA2OX8*, *KS3*, *PIN1* and *PIN11*, indicating that the QTL results of this study were highly reliable (Tudroszen et al., 1977; Winkler and Helentjaris,1995; Lo et al.,2008; Yamaguchi, 2008; Li et al., 2016; Weijers et al., 2018). Furthermore, 55% of QTLs were newly identified in the present study, including traits related to plant height and growth rate. Combining a large number of validated and new QTLs, we can discover the genetic basis affecting the dynamic development of plant height.

First, plant height at different stages was controlled by different QTLs. There were 6, 6, 2 and 24 loci detected for PH traits at the V5, V10, V12 and R stages, respectively (Fig.5; Data S1). More QTLs at the flowering stage were detected than at other stages. However, comparison of the QTLs for the four developmental stages did not show any overlapping regions, suggesting that plant height was controlled by different genes at different stages. For example, at the V5 stage, the gene *PIN1*, an

auxin transport protein (Kumari et al., 2015), was detected near to the QTL of chr9: 3.23-3.43Mb for the TEM group. The expression profile of *PIN1* in B73 showed high expression in the early stem, indicating that the gene may involve in the early stages of development. At the R stage, the gene *PIN11* which is an auxin efflux carrier family protein (Tudroszen et al., 1977; Balzan et al., 2014), was detected in the QTL of chr2:192.33-192.53Mb for the TEM group. The expression profile of *PIN11* for B73 showed that the gene expressed highly in the SAM and internode, indicating that the gene was likely to have controlled plant height, especially in later development.

Second, different QTLs controlled plant height in different groups. We found that few QTLs for the three populations overlapped in the same stage. For the PH trait across four stages, there were more QTLs detected in the other two groups than BOTH group except in the first stage (Fig. 6). The reason may be different GWAS model used for the three groups, and the model used for BOTH group was strict than the other two groups with population structure be considered. In addition, for the similar model of TEM and TST groups, the QTLs were still different, which may be caused by the allele frequencies. For example, the QTL chr2: 192.33-192.53 Mb (containing *PIN11*) was only detected in the TEM group at the R stage. The allele frequencies of the peak SNP (chr2.S_192432591, A/G) were 0.52/0.47 in the TEM group, 0.16/0.85 in the TST.

Third, we have found considerable overlap between PH, IPH, GRPH, IDPH and DGRPH (Fig. 7; Fig. S5). Based on the correlations between the five class traits, and the results of co-localization of QTLs, we can obtain a systematic understanding of the genetic basis of traits. For example, the QTL region chr2:2.49-4.36 Mb was co-located by PH_4, IPH_3t4 and GRPH_3t4, which contained the auxin corresponding factor gene *ARFTF4* (Auxin response factor 4; Li et al., 2016), indicating that the plant height at the R stage was mainly contributed by the difference of the growth rate of V12 to R stages rather than other periods. These results indicate that the plant height surveyed at a specific stage was affected by many factors, such as IPH and the plant height at the former stage.

Discussion

High-throughput phenotyping platforms promote genetic research

Application of genetic improvement is the most effective way to increase crop yields. With the fast development of sequencing technology, genomic researches have

recently been rapidly increasing; however, the phenotype has been facing bottleneck (Furbank and Tester, 2011). The development of HTPPs to obtain more phenotypes has been the focus of the fast development of genetics and breeding.

A series of indoor phenotypic platforms have recently been developed and applied into genetic researches (Chen et al., 2014; Yang et al., 2014; Zhang et al., 2016). The application of these high-throughput, automated phenotyping devices can greatly shorten the phenotypic investigation time, ensure the accuracy of the phenotype, and discover phenotypes that researchers cannot obtain by conventional techniques. More importantly, the traits discovered by the high throughput platform can identify some known genes as well as the novel loci, providing a valuable ability for gene identification.

Compared with indoor platforms, the development of field HTPPs will be much more complex because of the requirement for high flexibility and a large payload (Araus and Cairns, 2014). To date, UAV has been an excellent tool as field high-throughput techniques, and has achieved great success in the researches of wheat and cotton (Andrade-Sanchez et al., 2013; Holman et al., 2016). However, the applications for UAV in maize plant height research were very few. In this study, we applied the UAV platform to survey maize plant height in the fields and used the resultant accurate data for genetic mapping. A large number of reported and many novel QTLs were detected, showing the advantage of GWAS using the UAV-HTPPs in mining of plant height loci. The platform is likely to have a wide range of future applications and can be extended to more complex agronomic traits.

Dynamic phenotype accelerates the dissection of the genetic basis of plant height

The determination of plant height variation depends on the in-depth investigation of phenotype. Currently, the survey of plant height typically takes place at the mature stage, which can obtain stable traits, but a lot of useful plant height information is likely to be missed. In this study, we monitored the plant height from the seeding stage to the flowering stage, through division into four periods. We found that GRPH of maize varies greatly at different stages of development, with the fastest in 1t2 stage, and slowest in 3t4 stage. Second, we found that TST maize grew slower and had a shorter plant height than the TEM maize from sowing to jointing stage. However, from the jointing to the flowering stages, TST maize had a faster growth rate, and finally resulted in a taller plant than TEM maize. Third, there were different genes

regulating the plant height at different stages, some controlling early growth, some controlling mid-term and some controlling later stages. In this study we have detected 6, 6, 2 and 24 QTLs for the PH traits at V5, V10, V12 and R stages, but no common QTLs among the four stages. The results were consistent with Yan (Yan et al., 2003), who investigated plant heights in five periods and found that QTLs controlling plant heights were expressed differently in different periods. The above results indicate that if we assess the plant height over different growth stages, we will be able to identify more genes affecting plant height. Fourth, we found that a few regions can be co-localized by PH, IPH and GRPH. For example, we found that the co-localized QTLs controlling later IPH or GRPH were also detected in later PH traits and vice versa. This indicates that by dividing the plant height into several stages of growth, the key factors for the plant height can be better identified at specific stages. The dynamic phenotype enables us to have a clearer understanding of plant developmental processes. The usage of dynamic phenotypic data for mapping can identify more QTLs affecting the development of the trait, which is of great importance for the analysis of the genetic basis of traits and subsequent improvement of the trait.

Acknowledgements

The authors are grateful to Dr. Jianbing Yan for providing the maize natural population. Thank Dr. Boxiang Xiao for the software of Maize Three-Dimensional Interactive Digital Design (PlantCAD-maize) which helps to design the digital maize plants.

Author contributions

Y.X.Zhao, G.J.Y, and J.R.Z designed the experiment; R.Y.Z, X.S, K.C and Y.X.Zhang carried out the field experiment; G.J.Y and L.H conducted the UAV-HTTP. X.Q.W implement the statistical analysis and GWAS work. X.Q.W and Y.X.Zhao prepared the initial draft. X.L.L, M.J.L and W.S helped to modify the manuscript. J.R.Z and W.S provide the foundation support. All authors reviewed the manuscript.

Funding

This research was supported by funding from the National Key Research and Development Program of China (2016YFD0300106); the Science and Technology Planning Project of Beijing (D161100005716002); the Sci-Tech Innovative Ability Project (KJCX20170423); the Innovative Team Construction Project of BAAFS (JNKYT201603), China Agriculture Research System (CARS-02-11); the Beijing Scholars Program (BSP041).

Competing interests

The authors declare no competing financial interests.

References

Abendroth L, Elmore RW, Boyer M, Marlay SK. 2011. Corn growth and development. Iowa State University.

Al-Tamimi N, Brien C, Oakey H, Berger B, Saade S, Ho YS, Schmöckel SM, Tester M, Negrão S. 2016. Salinity tolerance loci revealed in rice using high-throughput non-invasive phenotyping. Nature Communications **17**, 13342.

Andradesanchez P, Gore MA, Heun JT, Thorp KR, Carmosilva AE, French AN, Salvucci ES, White JW. 2014. Development and evaluation of a field-based high-throughput phenotyping platform. Functional Plant Biology **41**, 68-79.

Araus JL, Cairns JE. 2014. Field high-throughput phenotyping: the new crop breeding frontier. Trends in Plant Science **19**, 52-61.

Balzan S, Johal GS, Carraro N. 2014. The role of auxin transporters in monocots development. Frontiers in Plant Science **15**, 393.

Bensen RJ, Johal GS, Crane VC, Tossberg JT, Schnable PS, Meeley RB, Briggs SP. 1995. Cloning and characterization of the maize An1 gene. Plant Cell **7**, 75-84.

Bendig J, Bolten A, Bareth G. 2013. UAV-based imagzing for multi-temporal, very high resolution crop surface models to monitor crop growth variability. Photogrammetrie-Fernerkundung-Geoinformation **6**, 551-562.

Chen D, Neumann K, Friedel S, Kilian B, Chen M, Altmann T, Klukas C. 2014. Dissecting the phenotypic components of crop plant growth and drought responses based on high-throughput image analysis. Plant Cell **26**, 4636-55.

Cristian F, Silvia F, and Serena V. 2012. The Maize PIN Gene Family of Auxin Transporters. Frontiers in Plant Science **3**, 16.

Dell'Acqua M, Gatti DM, Pea G, *et al*. 2015. Genetic properties of the MAGIC maize population: a new platform for high definition QTL mapping in Zea mays. Genome Biology **16**, 167.

Deng M, Li D, Luo J, Xiao Y, Liu H, Pan Q, Zhang X, Jin M, Zhao M, Yan J. 2017. The genetic architecture of amino acids dissection by association and linkage analysis in maize. Plant Biotechnology Journal **15**, 1250-1263.

Duan T, Zheng B, Guo W, Ninomiya S, Guo Y, Chapman SC. 2017. Comparison of ground cover estimates from experiment plots in cotton, sorghum and sugarcane based on images and ortho-mosaics captured by UAV. Functional Plant Biology **44**,169-183.

Fujioka S, Yamane H, Spray CR, Gaskin P, Macmillan J, Phinney BO, Takahashi N. 1988. Qualitative and quantitative analyses of gibberellins in vegetative shoots of normal, dwarf-1, dwarf-2, dwarf-3, and dwarf-5 seedlings of Zea mays L. Plant Physiology **88**,1367-72.

Furbank RT, Tester M. 2011. Phenomics--technologies to relieve the phenotyping

bottleneck. Trends in Plant Science **16**, 635-44.

Heuer S, Hansen S, Bantin J, Brettschneider R, Kranz E, Lörz H, Dresselhaus T. 2001. The maize MADS box gene ZmMADS3 affects node number and spikelet development and is co-expressed with ZmMADS1 during flower development, in egg cells, and early embryogenesis. Plant Physiology **127**, 33-45.

Holman F, Riche A, Michalski A, Castle M, Wooster M, Hawkesford M. 2016. High throughput field phenotyping of wheat plant height and growth rate in field plot trials using UAV based remote sensing. Remote Sensing of Environment **8**, 1031.

Hoffmeister D, Bolten A, Curdt C, Waldhoff G, Bareth G. 2010. High-resolution Crop Surface Models (CSM) and Crop Volume Models (CVM) on field level by terrestrial laser scanning. International Society for Optics and Photonics **7840**, 78400E.

Hoffmeister D, Waldhoff G, Curdt C, Tilly N, Bendig J, Bareth G. 2013. Spatial variability detection of crop height in a single field by terrestrial laser scanning. In Precision agriculture'13. Wageningen Academic Publishers, Wageningen, 267-274.

Hung HY, Shannon LM, Tian F, *et al*. 2012. ZmCCT and the genetic basis of day-length adaptation underlying the postdomestication spread of maize. Proceedings of the National Academy of Sciences of the United States of America **109**, 1913-1921.

Juarez MT, Kui JS, Thomas J, Heller BA, Timmermans MC. 2004. microRNA mediated repression of rolled leaf1 specifies maize leaf polarity. Nature **428**, 84-8.

Khush GS. 2001. Green revolution: the way forward. Nature Reviews Genetics **2**, 815-22.

Li SB, Xie ZZ, Hu CG, Zhang JZ. 2016. A review of auxin response factors (ARFs) in plants. Frontiers in Plant Science **3**, 7:47

Liang Z, Pandey P, Stoerger V, Xu Y, Qiu Y, Ge Y, Schnable JC. 2018. Conventional and hyperspectral time-series imaging of maize lines widely used in field trials. Gigascience **7**, 1-11.

Liu H, Wang X, Warburton ML, *et al*. 2015. Genomic, transcriptomic, and phenomic variation reveals the complex adaptation of modern maize breeding. Molecular Plant **8**, 871-884.

Liu H, Luo X, Niu L, *et al*. 2017. Distant eQTLs and Non-coding Sequences Play Critical Roles in Regulating Gene Expression and Quantitative Trait Variation in Maize. Molecular Plant **6**, 414-426.

Liu X, Huang M, Fan B, Buckler ES, Zhang Z. 2016. Iterative usage of fixed and random effect models for powerful and efficient genome-wide association studies. PLoS Genetics **12**, e1005767.

Lo SF, Yang SY, Chen KT, Hsing YI, Zeevaart JA, Chen LJ, Yu SM. 2008. A novel class of gibberellin 2-oxidases control semidwarfism, tillering, and root development in rice. Plant Cell **20**, 2603-18.

Mizutani M. 2012. Impacts of diversification of cytochrome P450 on plant metabolism. Biological & Pharmaceutical Bulletin **35**, 824-32.

Pan Q, Xu Y, Li K, Peng Y, Zhan W, Li W, Li L, Yan J. 2017. The Genetic Basis of Plant Architecture in 10 Maize Recombinant Inbred Line Populations. Plant Physiology **175**, 858-873.

Peiffer JA, Romay MC, Gore MA, *et al*. 2014. The genetic architecture of maize height. Genetics **196**, 1337-56.

Peng J, Richards DE, Hartley NM, *et al*. 1999. 'Green revolution' genes encode mutant gibberellin response modulators. Nature **15**, 256-61.

Salas Fernandez MG, Becraft PW, Yin Y, Lübberstedt T. 2009. From dwarves to giants? Plant height manipulation for biomass yield. Trends in Plant Science **14**, 454-61.

Sasaki A, Ashikari M, Ueguchi-Tanaka M, *et al*. 2002. Green revolution: a mutant gibberellin-synthesis gene in rice. Nature **18**, 701-2.

Schoof H, Lenhard M, Haecker A, Mayer K F, Jürgens G, Laux T. 2000. The stem cell population of Arabidopsis shoot meristems in maintained by a regulatory loop between the CLAVATA and WUSCHEL genes. Cell **100**, 635-44.

Sharma VK, Carles C, Fletcher JC. 2003. Maintenance of stem cell populations in plants. Proceedings of the National Academy of Sciences of the United States of America **100**, 11823–11829.

Tester M, Langridge P. 2010. Breeding technologies to increase crop production in a changing world. Science **12**, 818-22.

Tudroszen NJ, Kelly DP, Millis NF. 1977. alpha-Pinene metabolism by Pseudomonas putida. Biochemical Journal **15**, 315-8.

van Heerwaarden J, Doebley J, Briggs WH, Glaubitz JC, Goodman MM, de Jesus Sanchez Gonzalez J, Ross-Ibarra J. 2011. Genetic signals of origin, spread, and introgression in a large sample of maize landraces. Proceedings of the National Academy of Sciences of the United States of America **18**, 1088-92.

Watanabe K, Guo W, Arai K, *et al*. 2017. High-throughput phenotyping of sorghum plant height using an unmanned aerial vehicle and its application to genomic prediction modeling. Frontiers in Plant Science **8**, 421.

Winkler RG, Freeling M. 1994. Physiological genetics of the dominant gibberellin-nonresponsive maize dwarfs, Dwarf8 and Dwarf9. Planta **193,** 341-348.

Wei X, Xu J, Guo H, Jiang L, Chen S, Yu C, Zhou Z, Hu P, Zhai H, Wan J. 2010. DTH8 suppresses flowering in rice, influencing plant height and yield potential simultaneously. Plant Physiology **153**, 1747-58.

Weijers D, Nemhauser J, Yang Z. 2018. Auxin: small molecule, big impact. Journal of Experimental Botany **69**, 133-136.

552 **Winkler RG, Helentjaris T**. 1995. The maize Dwarf3 gene encodes a cytochrome
553 P450-mediated early step in gibberellin biosynthesis. Plant Cell **7**, 1307-17.
554 **Woebbecke DM, Meyer GE, Von Bargen K, Mortensen DA**. 1995. Color indices for weed
555 identification under various soil, residue, and lighting conditions. Transactions of the ASAE,
556 **38**, 259-269.
557 **Xing A, Gao Y, Ye L, *et al***. 2015. A rare SNP mutation in Brachytic2 moderately reduces
558 plant height and increases yield potential in maize. Journal of Experimental Botany **66**,
559 3791-802.
560 **Yamaguchi S**. 2008. Gibberellin metabolism and its regulation. Annual Review of Plant
561 Biology **59**, 225-251.
562 **Yan J, Tang H, Huang Y, Shi Y, Li J, Zheng Y**. 2003. Dynamic analysis of QTL for plant
563 height at different developmental stages in maize (*Zea mays* L.). Chinese Science Bulletin **48**,
564 2601-2607.
565 **Yang N, Lu Y, Yang X, Huang J, Zhou Y, Ali F, Wen W, Liu J, Li J, Yan J**. 2014. Genome
566 wide association studies using a new nonparametric model reveal the genetic architecture of
567 17 agronomic traits in an enlarged maize association panel. PLoS Genetics, **10**, e1004573.
568 **Yang X, Gao S, Xu S, Zhang Z, Prasanna BM, Li L, Li J, Yan J**. 2011. Characterization of
569 a global germplasm collection and its potential utilization for analysis of complex quantitative
570 traits in maize. Molecular Breeding **28**, 511-526.
571 **Yang W, Guo Z, Huang C, *et al***. 2014. Combining high-throughput phenotyping and
572 genome-wide association studies to reveal natural genetic variation in rice. Nature
573 Communications **8**, 5087.
574 **Zhang J, Cheng Z, Zhang R**. 2012. Regulated deficit drip irrigation influences on seed
575 maize growth and yield under film. Procedia Engineering **28**, 464-468.
576 **Zhou Z, Zhang C, Zhou Y, *et al***. 2016. Genetic dissection of maize plant architecture with
577 an ultra-high density bin map based on recombinant inbred lines. BMC Genomics **3**, 178.
578
579
580
581
582
583
584
585
586
587
588

589 **Table 1** . The investigation date for plant height

Flight	Date	DAS[a]	DAFD[b]	Development stage	Description
1	8 June 2017	24	—	V5	seeding stage
2	29 June 2017	45	21	V10	jointing stage
3	11 July 2017	57	12	V12	trumpet
4	3 August 2017	80	23	R	flowering stage

590 Note:

591 a: DAS means days after sowing

592 b: DAFD means days after the closest former date

593

594 **Table 2.** Features for the extraction for the plant height using UAV-HTTP

Flight	Flight Altitude (m)	Original images quantity	Checked images quantity	Orthomosaic Resolution (cm/pixel)	Point Density (points/cm-2)	DSM Resolution (cm/pixel)	Min of CSM (cm)	Max of CSM (cm)	CV of CSM (%)	Mean of CSM(cm)
1	40	166	120	0.72	47.9	1.44	0	26	53	9.6
2	60	113	98	1.33	14.2	2.65	69	184	13.4	124.9
3	60	121	95	1.35	13.7	2.71	117	251	11.6	185.9
4	50	159	147	1.23	16.4	2.47	148	365	14.5	253.4

595

596 **Table 3.** Statistic analysis for plant height variation for the whole population during
597 four growth stages

Trait	Max (cm)	Min (cm)	Mean (cm)	Sd (cm)	CV (%)
PH_1	31.34	5.35	13.66	5.07	37.09
PH_2	149.99	54.28	90.42	15.46	17.1
PH_3	212.56	96.52	146.98	22.63	15.4
PH_4	325.01	112.9	218.26	35.58	16.3
IPH_1t2	125.98	44.45	77.35	13.59	17.57
IPH_2t3	89.79	11.25	56.85	14.54	25.58
IPH_3t4	153.81	0.26	71.57	32.76	45.78
DIPH_1t2	6	2.12	3.68	0.65	17.57
DIPH_2t3	7.48	0.94	4.74	1.21	25.58
DIPH_3t4	6.69	0.01	3.11	1.42	45.78
GRPH_1t2	16.05	2.26	6.47	2.7	41.75
GRPH_2t3	1.32	0.12	0.64	0.18	28.47
GRPH_3t4	1.27	0	0.51	0.25	49.61
DGRPH_1t2	0.76	0.11	0.31	0.13	41.75
DGRPH_2t3	0.11	0.01	0.05	0.02	28.47
DGRPH_3t4	0.06	0	0.02	0.01	49.61

598
599

Figure legends

Fig. 1 Field high-throughput phenotyping for plant height. A, digital designed graphs for the maize plants during the four stages. B, the UAV equipment and the plant height extraction process. The main process contained the image collection by the UAV, then divided the pictures into the mosaic plots, and extracted plant height based on the formula (CSM=DSM-DEM). C, Dynamic plant height and QTL dissection. The whole procedure included trait variation and correlation analysis, as well as GWAS.

Fig. 2 Linear relationship for plant height by UVA and manual measurement by ruler at three growth stages. The blue solid line represents the regression line, and the grey shadow represents the 99% confidence interval.

Fig. 3 Correlation coefficient matrix among 16 plant-height-related traits. Yellow and blue indicate positive and negative correlations, respectively, and the size of the circle is proportional to the correlation coefficient. The number indicates the correlation coefficient.

Fig. 4 Plant height and its related trait variations between the TEM and TST populations at four growth stages. Blue and red represent the TEM and TST populations, respectively. The line in the box plots show the median value. Box edges represent the first and third quartiles, and the dots outside the whiskers represent the value over 1.5 × interquartile range. Stars means phenotypic distribution has significantly difference below 0.05.

Fig. 5 Genome-wide association study for the plant heights at the four stages among the TEM, TST and BOTH groups. Different colors represent different chromosomes. The dotted line is the threshold. SNPs above the threshold showed significant association ones.

Fig. 6 Number of QTL for plant height among the three groups (TEM, TST and BOTH) for four stages. A, the number and proportion of QTLs for the three groups. B, the QTLs for each group at each of the four stages.

634 **Fig. 7 The venn graph of QTLs for PH, IPH and GRPH traits.**

635

636

A The 4 growth stages for maize

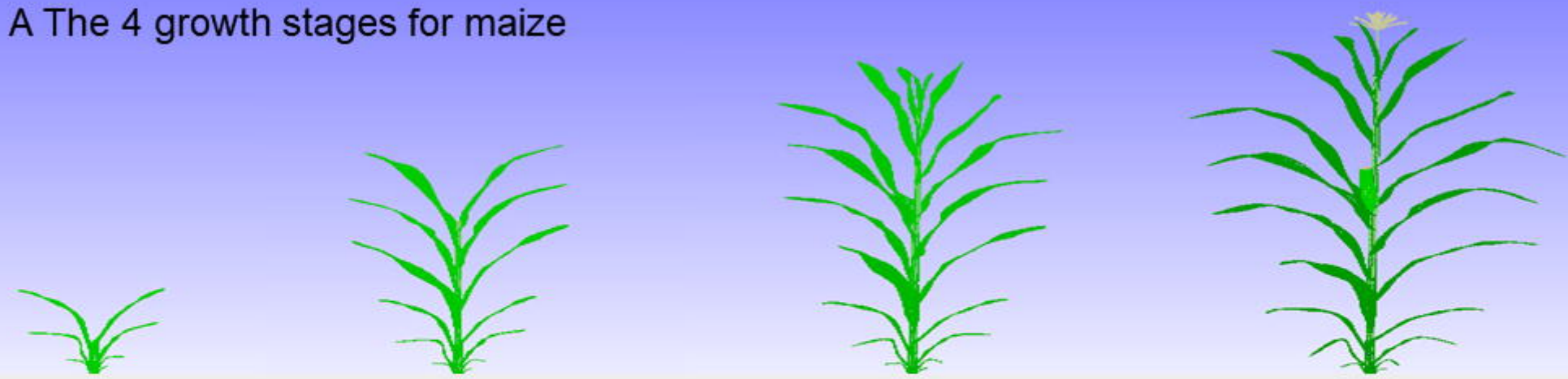

B UAV and the plant height extraction process

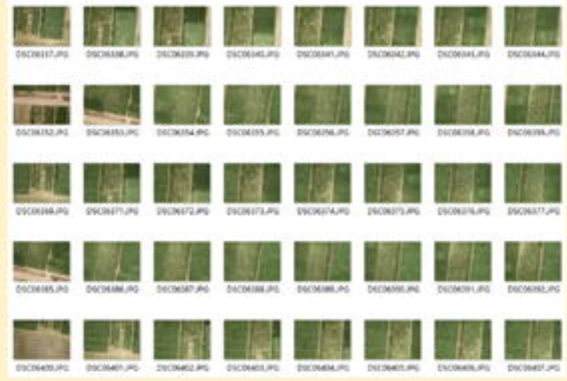

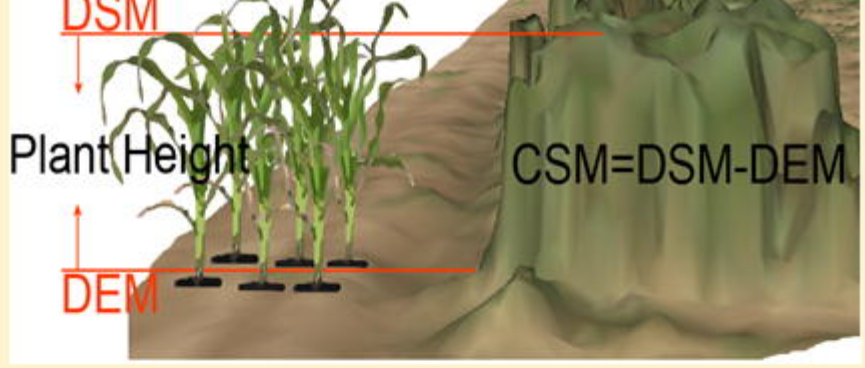

C Dynamic plant height and its QTL dissection

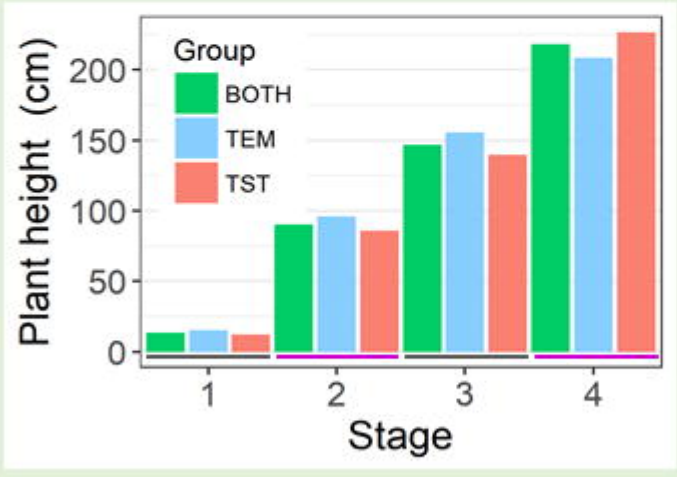

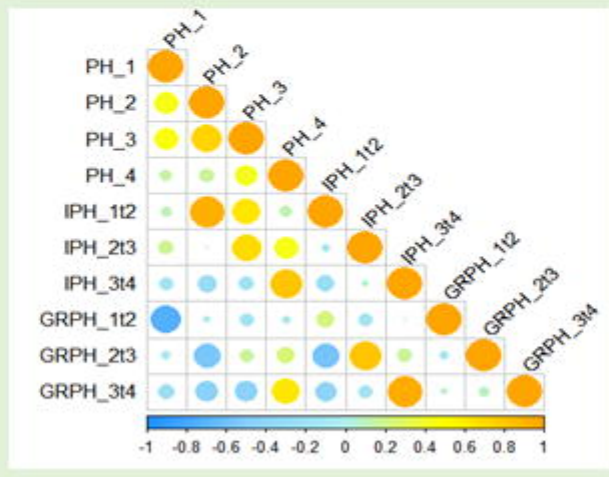

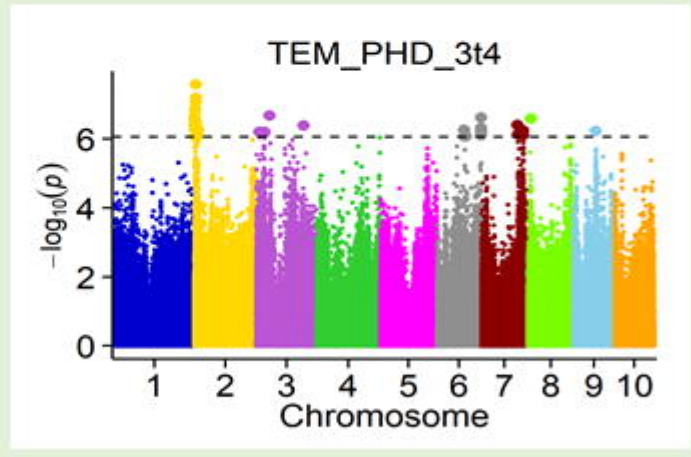

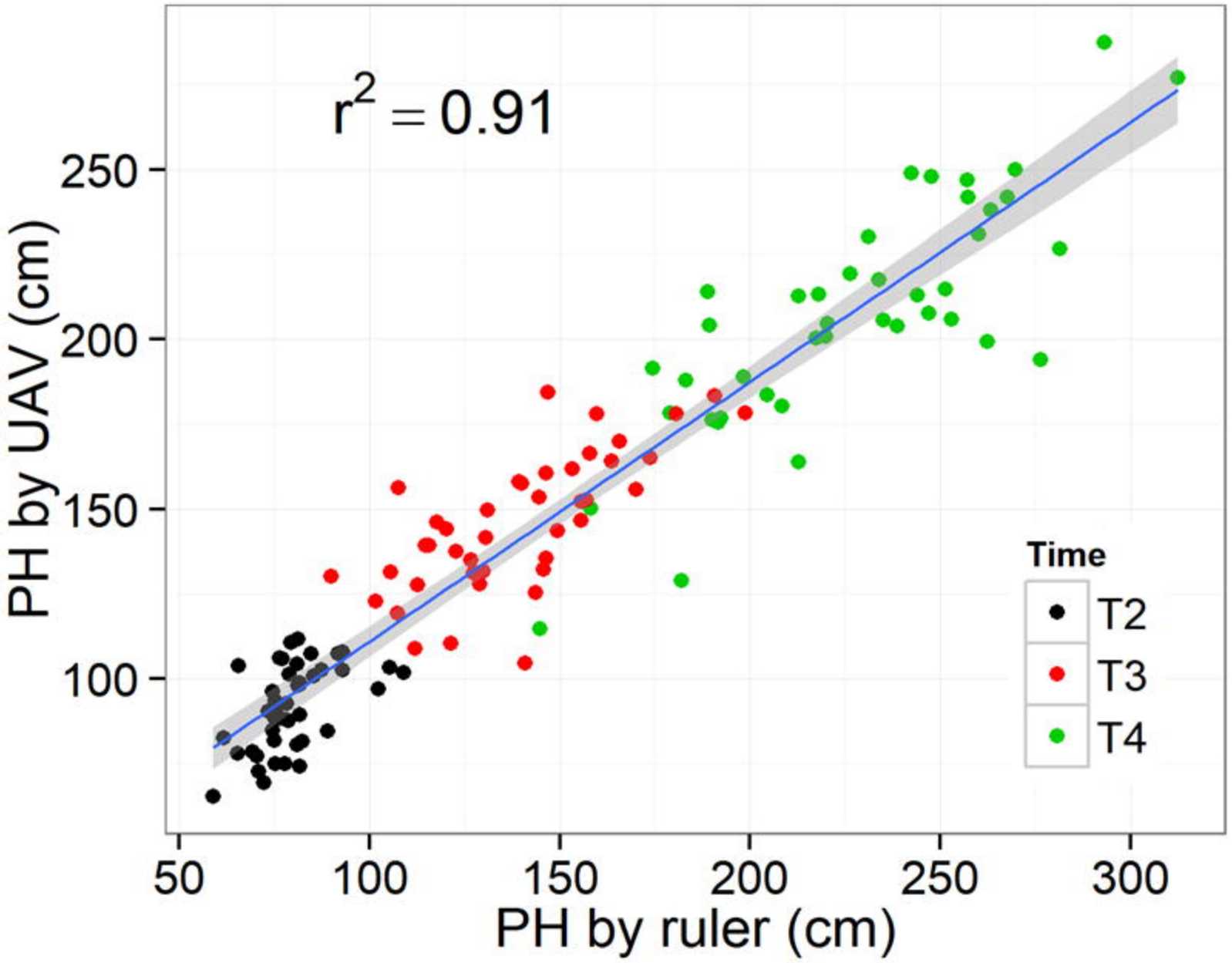
$r^2 = 0.91$
PH by UAV (cm)
250
200
150
100
50
100
150
200
250
300
PH by ruler (cm)
Time
T2
T3
T4

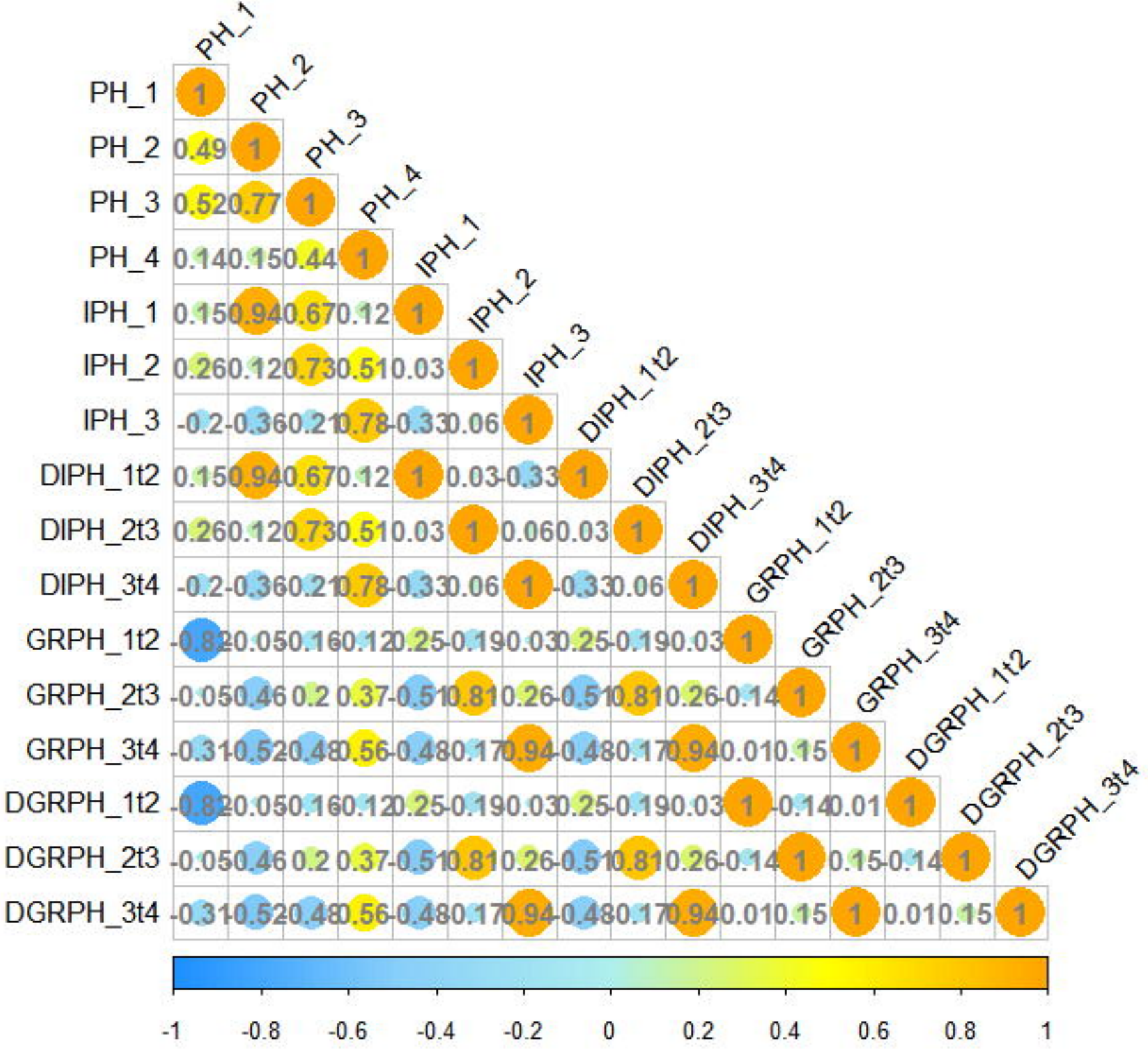
PH_1
PH_2
PH_3
PH_4
IPH_1
IPH_2
IPH_3
DIPH_1t2
DIPH_2t3
DIPH_3t4
GRPH_1t2
GRPH_2t3
GRPH_3t4
DGRPH_1t2
DGRPH_2t3
DGRPH_3t4
1 0.49 1 0.52 0.77 1 0.14 0.15 0.44 1 0.15 0.94 0.67 0.12 1 0.26 0.12 0.73 0.51 0.03 1 -0.2 -0.36 0.21 0.78 -0.33 0.06 1 0.15 0.94 0.67 0.12 1 0.03 -0.33 1 0.26 0.12 0.73 0.51 0.03 1 0.06 0.03 1 -0.2 -0.36 0.21 0.78 -0.33 0.06 1 -0.33 0.06 1 -0.82 0.05 0.16 0.12 0.25 -0.19 0.03 0.25 -0.19 0.03 1 -0.05 0.46 0.2 0.37 -0.51 0.81 0.26 -0.51 0.81 0.26 -0.14 1 -0.31 0.52 0.48 0.56 -0.48 0.17 0.94 -0.48 0.17 0.94 0.01 0.15 1 -0.82 0.05 0.16 0.12 0.25 -0.19 0.03 0.25 -0.19 0.03 1 -0.14 0.01 1 -0.05 0.46 0.2 0.37 -0.51 0.81 0.26 -0.51 0.81 0.26 -0.14 1 0.15 -0.14 1 -0.31 0.52 0.48 0.56 -0.48 0.17 0.94 -0.48 0.17 0.94 0.01 0.15 1 0.01 0.15 1
-1 -0.8 -0.6 -0.4 -0.2 0 0.2 0.4 0.6 0.8 1

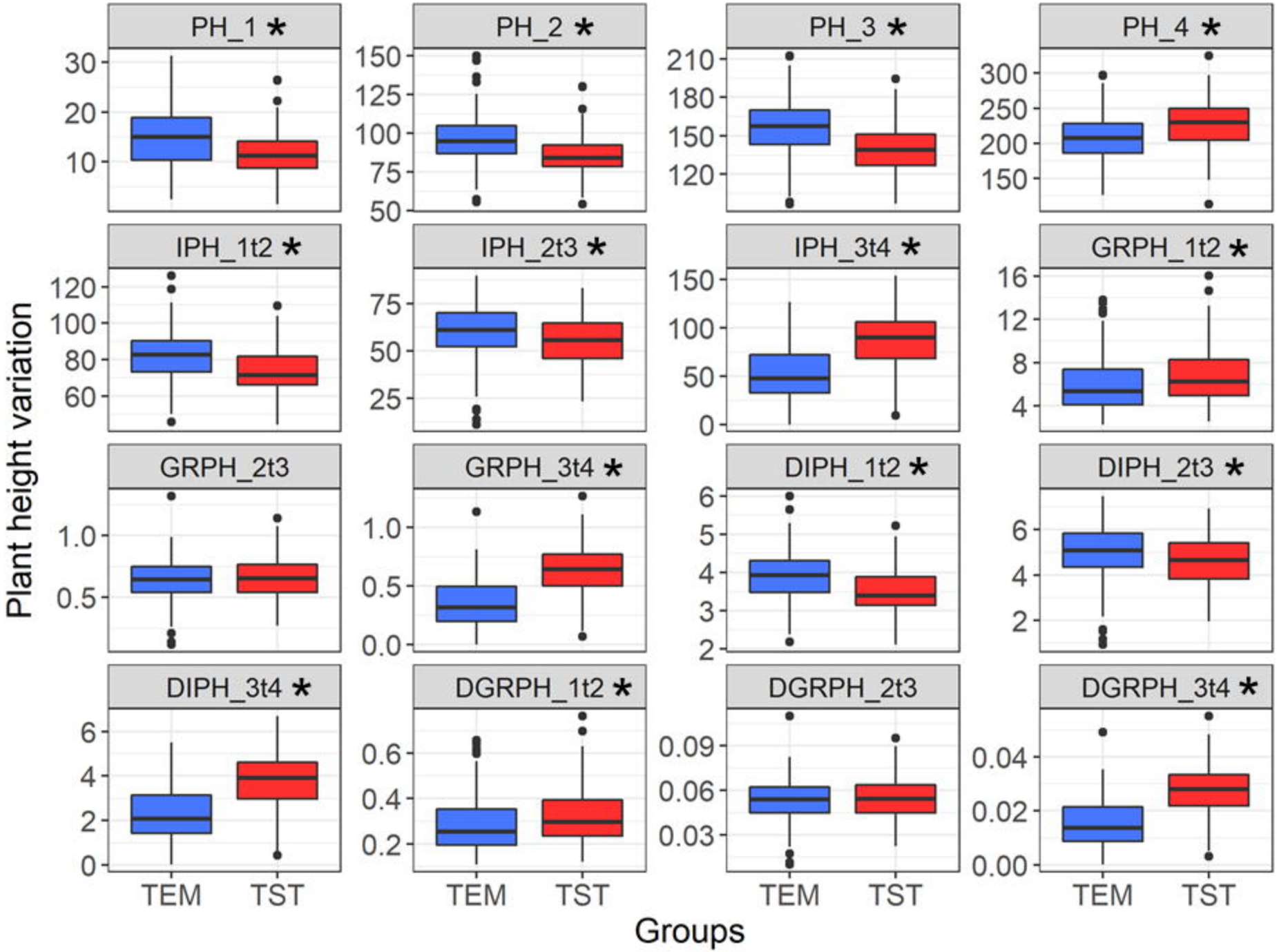
PH_1 *
PH_2 *
PH_3 *
PH_4 *
IPH_1t2 *
IPH_2t3 *
IPH_3t4 *
GRPH_1t2 *
GRPH_2t3
GRPH_3t4 *
DIPH_1t2 *
DIPH_2t3 *
DIPH_3t4 *
DGRPH_1t2 *
DGRPH_2t3
DGRPH_3t4 *
Plant height variation
TEM
TST
Groups

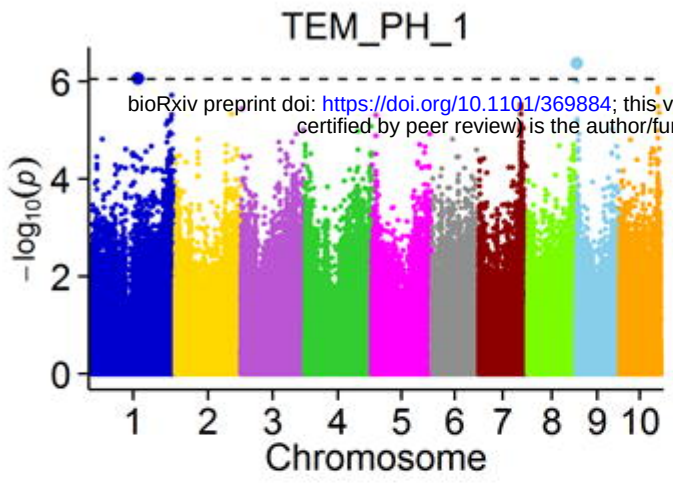

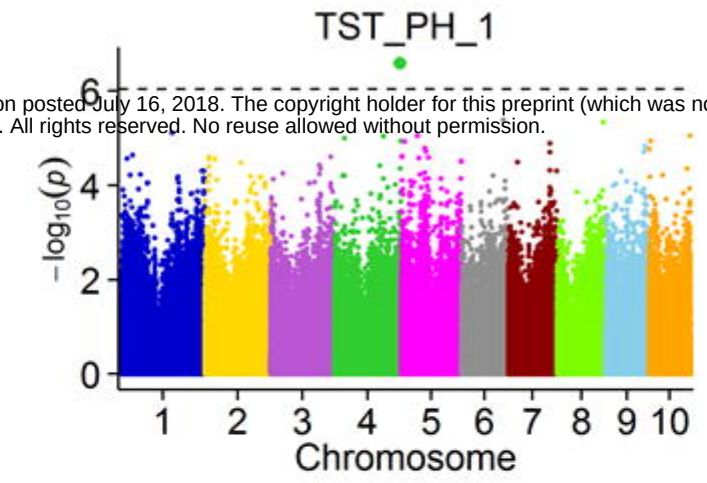

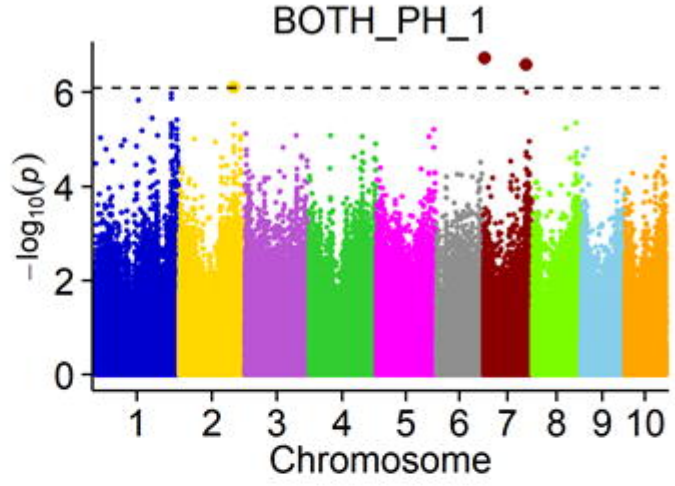

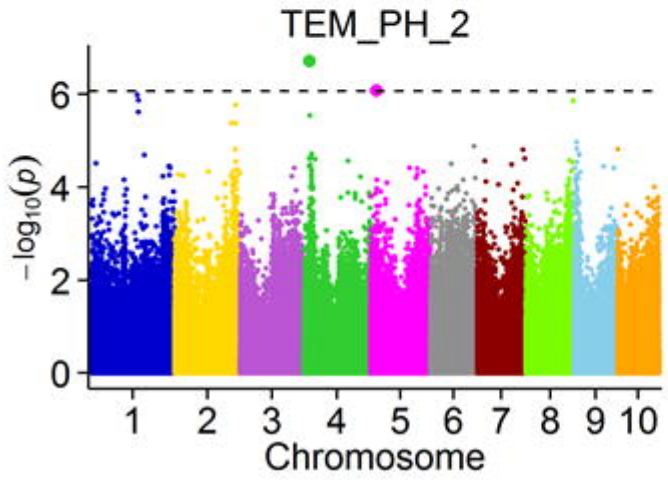

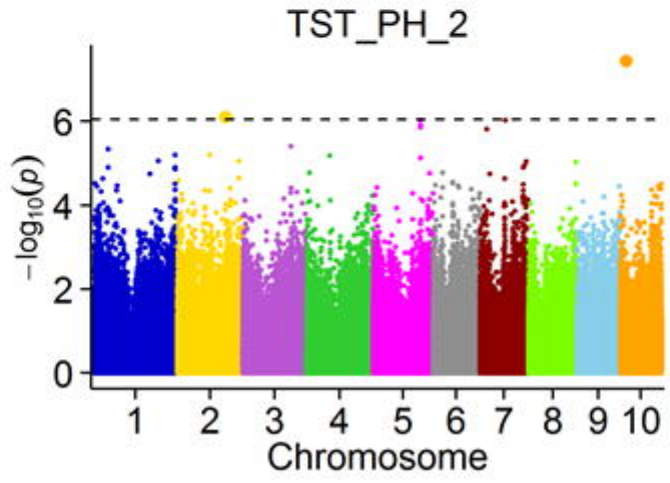

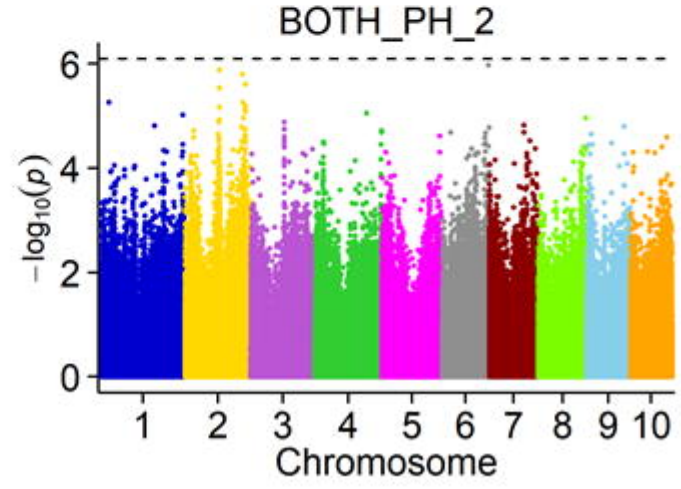

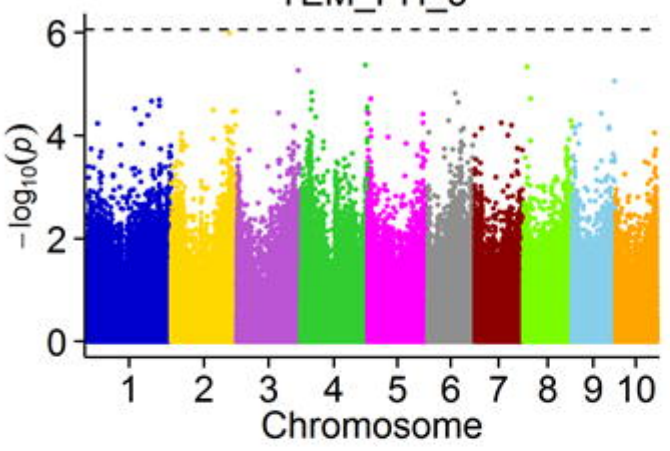

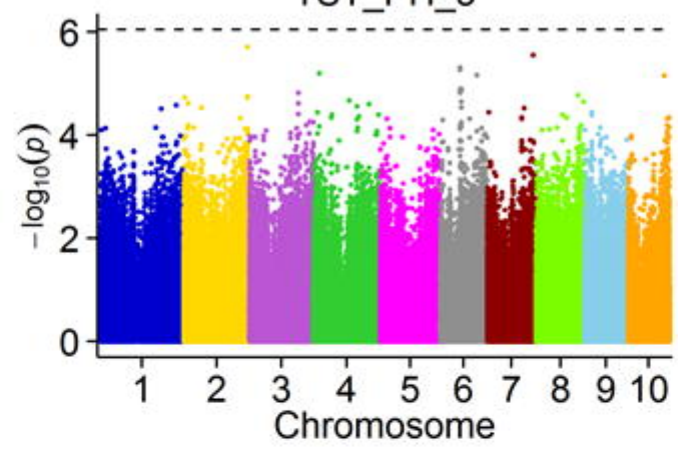

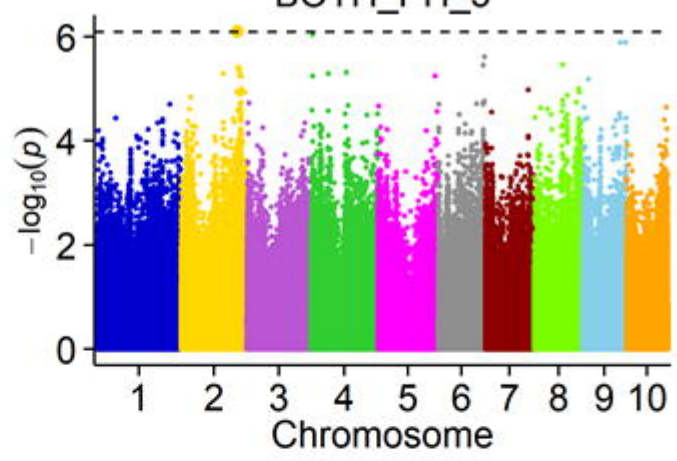

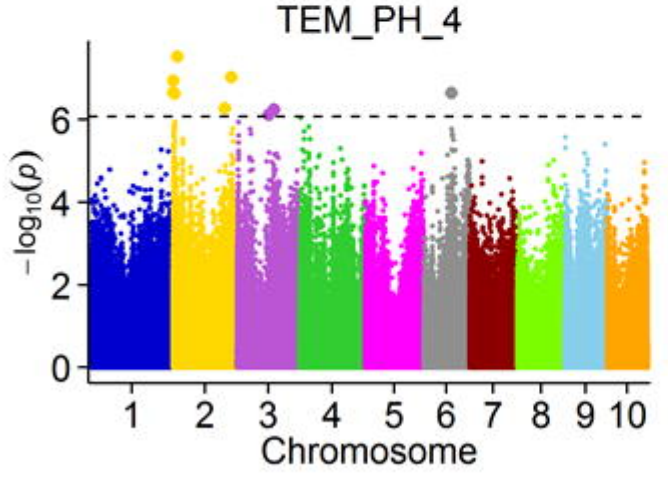

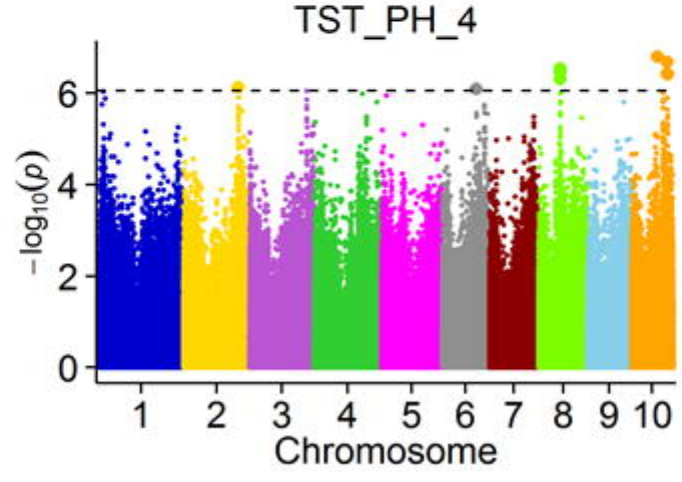

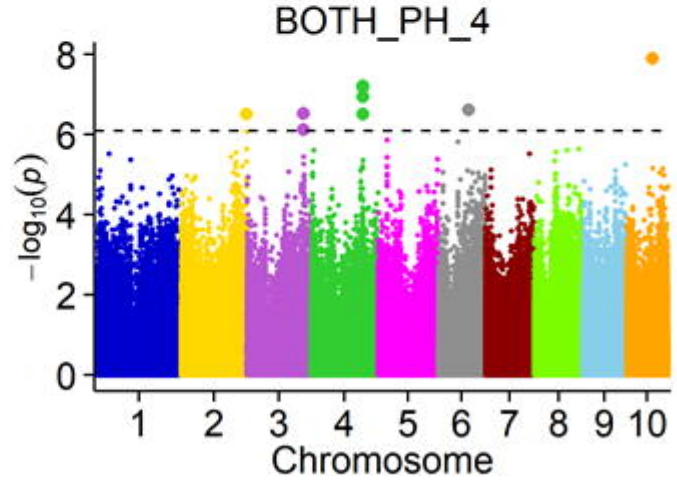

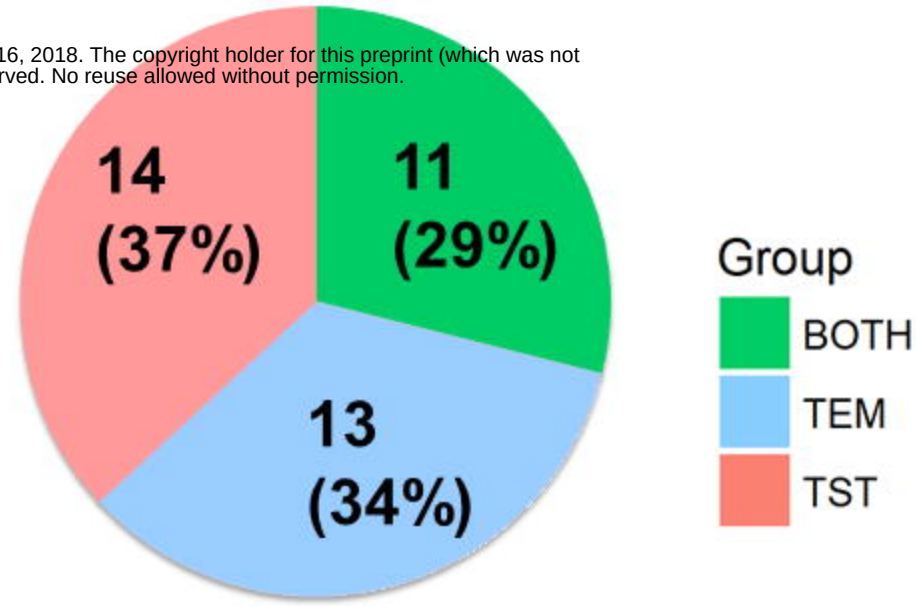

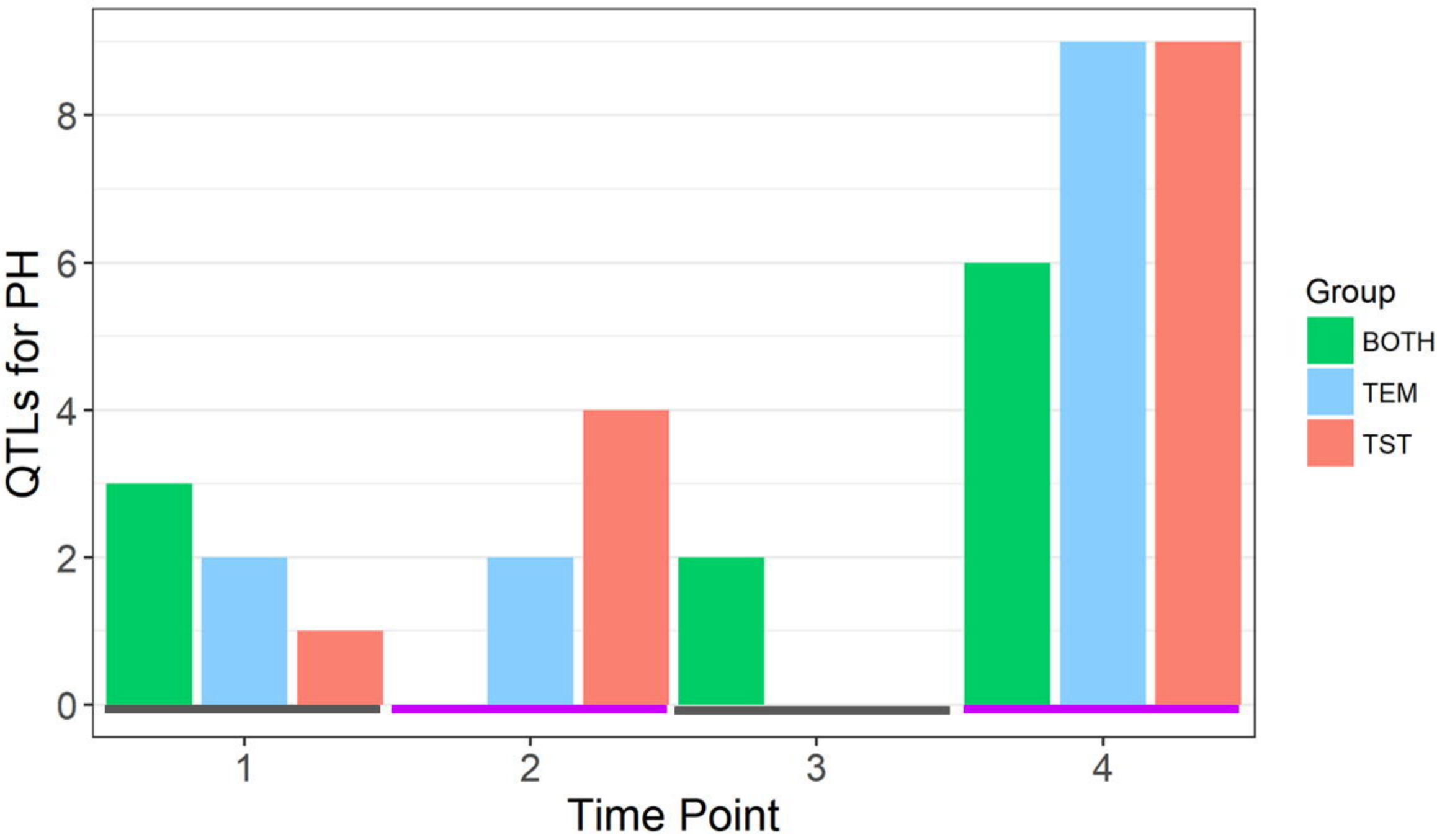

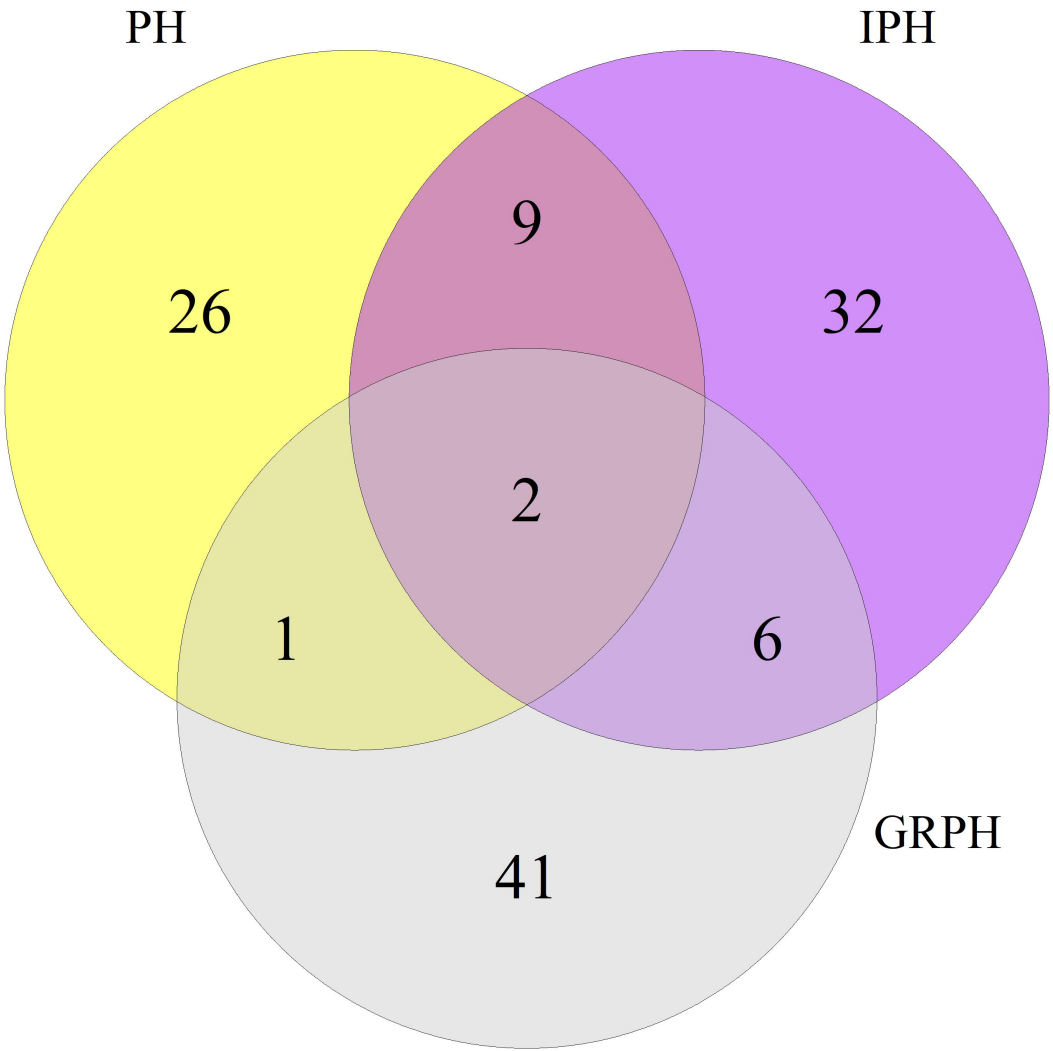
PH
IPH
GRPH
26
9
32
2
1
6
41